

A proposal for 4-D seismic imaging

Jeroen Beishuizen, Menno Dillen, Jacob Fokkema, Kees Wapenaar
Centre for Technical Geoscience, Delft University of technology*

Summary

Up to this point the results of the 4-D experiment have been employed to produce a difference dataset from the survey at the start and the one after a certain time span. Then from this difference conclusions are drawn with respect to the medium change. In this paper a reciprocity theorem is employed to derive the volume integral representation, which shows how this difference is related to the restricted area where the changes occur. This formulation is suited for inversion. Using the boundary integral representation we arrive at an operational procedure for 4-D prestack imaging.

Introduction

Seismic imaging and characterization is concerned with the use of sound waves to delineate contrasts in the medium parameters. Then following the standard analysis this contrast is associated with changes in the geological structure of the subsurface. The oil industry has successfully used this technique to delineate oil and gas fields. In the same spirit induced changes in the subsurface geology can also be detected if they can be related to a temporal change in the medium parameters. However, this is only true if the time rate of change is happening on a time scale which is much larger than the experiment time of a standard seismic survey. The seismic activity associated with this type of diagnosis is known as 4-D seismics or time-lapse seismics. Nur et al. [3] observed significant changes in the compressional wave speed in cores saturated with heavy oil as a function of the ambient temperature. From this observation he conjectured that seismic techniques could be used to monitor the thermal effect of injected steam to enhance the oil recovery of a reservoir. Not only thermal effects on wave propagation can be monitored. Cruts et al. [1] showed that induced stress in reservoir rock changes the anisotropy of rock parameters. This study is important for the gas-producing fields in the Northern part of the Netherlands. The hydrostatic pressure drop in the reservoir due to gas production induces subsidence and triggers small earth quakes. In this case 4-D seismics could be used to forecast the stress build-up in the medium and its geomechanical consequences.

The acoustic reciprocity formulation

In the acoustic reciprocity theorem two wave field states are distinguished. The states can be completely different, although they share the same spatial domain of application, \mathbb{D} , and they are related via an interaction quantity. The boundary surface of \mathbb{D} is denoted by Σ with the normal vector \mathbf{n} . The acoustic wave fields in the two states satisfy the following acoustic wave equation in

the frequency domain:

$$\partial_k \left(\frac{1}{\varrho} \partial_k P \right) + \omega^2 \kappa P = -j\omega Q, \quad (1)$$

where $P = P(\mathbf{x}, \omega)$ is the pressure, $\varrho = \varrho(\mathbf{x})$ is the mass density, $\kappa = \kappa(\mathbf{x})$ is the compressibility and $Q = Q(\mathbf{x}, \omega)$ is the volume density of injection rate. Einstein's summation convention applies to repeated subscripts. In the further analysis we will omit the explicit functional dependence on the circular frequency ω . The two different states are labeled by superscripts '0' and '1' for states 0 and 1, respectively. When we consider only contrast in the compressibility and different sources in \mathbb{D} , the global form of the reciprocity theorem reads

$$\begin{aligned} & \int_{\Sigma} \frac{1}{\varrho} (P^0 \partial_k P^1 - P^1 \partial_k P^0) n_k dA \\ &= \int_{\mathbb{D}} \omega^2 (\kappa^1 - \kappa^0) P^0 P^1 dV \\ &+ \int_{\mathbb{D}} j\omega (Q^1 P^0 - Q^0 P^1) dV, \end{aligned} \quad (2)$$

(see Fokkema and van den Berg [2]). We note that in the formulation of equation (2) the mass density is not different in the two states but has an inhomogeneous spatial character. In order to relate the reciprocity theorem with the 4-D seismic experiment we connect state 0 with the seismic situation at time instant $t = t_0$, which we call the reference state. State 1 is related with the situation at $t = t_1$, such that $t_1 > t_0$, which is known as the monitor state. In that case the reciprocity formulation describes the change in compressibility between t_0 and t_1 due to some geomechanical process or consequences of production activities. As far as the sources are concerned at the two time instants we consider the action of point sources that have the same wavelet spectrum S but, optionally, different spatial locations. In particular we have in state 0

$$j\omega Q^0(\mathbf{x}) = S \delta(\mathbf{x} - \mathbf{x}^S), \quad (3)$$

where the source position is taken as the actual source position in the seismic experiments. In state 1 the source term is written as

$$j\omega Q^1(\mathbf{x}) = S \delta(\mathbf{x} - \mathbf{x}^R), \quad (4)$$

where the 'source' position is taken at the actual receiver position in the seismic experiments. The corresponding wave fields in the two situations are written as $P^0 = P^0(\mathbf{x}|\mathbf{x}^S)$ and $P^1 =$

4-D imaging

$P^1(\mathbf{x}|\mathbf{x}^R)$ to relate them to their difference in spatial source positions. Where necessary the associated scalar Green's functions are introduced as

$$P^0(\mathbf{x}|\mathbf{x}^S) = G^0(\mathbf{x}|\mathbf{x}^S)S \quad \text{and} \quad P^1(\mathbf{x}|\mathbf{x}^R) = G^1(\mathbf{x}|\mathbf{x}^R)S. \quad (5)$$

Next we apply the reciprocity theorem of equation (2) to the domain \mathbb{R}^3 and relate the domain \mathbb{D} with the domain of the factual change in compressibility between the two time instants. Operating in this way we arrive at

$$\begin{aligned} S[P^1(\mathbf{x}^S|\mathbf{x}^R) - P^0(\mathbf{x}^R|\mathbf{x}^S)] \\ = \int_{\mathbb{D}} \omega^2 [\kappa^1(\mathbf{x}) - \kappa^0(\mathbf{x})] P^0(\mathbf{x}|\mathbf{x}^S) P^1(\mathbf{x}|\mathbf{x}^R) dV, \\ \text{with } \{\mathbf{x}^R, \mathbf{x}^S\} \in \mathbb{R}^3, \end{aligned} \quad (6)$$

where we used the fact that the boundary integral at infinity on the left-hand side of equation (2) vanishes due to the causality condition. After using physical reciprocity $P^1(\mathbf{x}^S|\mathbf{x}^R) = P^1(\mathbf{x}^R|\mathbf{x}^S)$ and introducing the difference wave field ΔP and the contrast parameter $\Delta\kappa$ as

$$\Delta P(\mathbf{x}^R|\mathbf{x}^S) = P^1(\mathbf{x}^R|\mathbf{x}^S) - P^0(\mathbf{x}^R|\mathbf{x}^S), \quad (7)$$

$$\Delta\kappa(\mathbf{x}) = \kappa^1(\mathbf{x}) - \kappa^0(\mathbf{x}), \quad (8)$$

equation (6) is compactly written as

$$\Delta P(\mathbf{x}^R|\mathbf{x}^S) = \int_{\mathbb{D}} \omega^2 \Delta\kappa(\mathbf{x}) G^0(\mathbf{x}|\mathbf{x}^S) P^1(\mathbf{x}|\mathbf{x}^R) dV, \quad (9)$$

where we used the Green's function definition for G^0 of equation (5). Equation (9) learns us how the *difference in wave fields* between t_1 and t_0 is related to the factual *difference in compressibility* for every receiver position \mathbf{x}^R and source position \mathbf{x}^S in \mathbb{R}^3 , provided that we take the same set $\{\mathbf{x}^R, \mathbf{x}^S\}$ at the different time instants. Besides the volume integral representation over the contrast domain \mathbb{D} , it is also possible to derive a boundary integral representation over the contrast surface Σ . To that end we apply the reciprocity theorem to \mathbb{D}' , the complement of the domain \mathbb{D} , and we arrive at

$$\begin{aligned} \Delta P(\mathbf{x}^R|\mathbf{x}^S) = \int_{\Sigma} \frac{1}{\varrho(\mathbf{x})} & \left[P^1(\mathbf{x}|\mathbf{x}^R) \partial_k G^0(\mathbf{x}|\mathbf{x}^S) \right. \\ & \left. - G^0(\mathbf{x}|\mathbf{x}^S) \partial_k P^1(\mathbf{x}|\mathbf{x}^R) \right] n_k dA. \end{aligned} \quad (10)$$

To have the *difference* wave field also in the integrand of the boundary integral at the right-hand side of equation (10) we use the reciprocity theorem for two situations of the wave field in state

0. As domain of application we take \mathbb{D}' and the source and receiver locations are taken in \mathbb{D}' as well. We have

$$\begin{aligned} & \int_{\Sigma} \frac{1}{\varrho(\mathbf{x})} \left[P^0(\mathbf{x}|\mathbf{x}^R) \partial_k G^0(\mathbf{x}|\mathbf{x}^S) \right. \\ & \left. - G^0(\mathbf{x}|\mathbf{x}^S) \partial_k P^0(\mathbf{x}|\mathbf{x}^R) \right] n_k dA \\ & = S[P^0(\mathbf{x}^S|\mathbf{x}^R) - P^0(\mathbf{x}^R|\mathbf{x}^S)] = 0, \end{aligned} \quad (11)$$

where we have used the physical reciprocity relation for the reference state. Then subtracting the result of equation (11) from equation (10) we arrive at

$$\begin{aligned} \Delta P(\mathbf{x}^R|\mathbf{x}^S) = \int_{\Sigma} \frac{1}{\varrho(\mathbf{x})} & \left[\Delta P(\mathbf{x}|\mathbf{x}^R) \partial_k G^0(\mathbf{x}|\mathbf{x}^S) \right. \\ & \left. - G^0(\mathbf{x}|\mathbf{x}^S) \partial_k \Delta P(\mathbf{x}|\mathbf{x}^R) \right] n_k dA. \end{aligned} \quad (12)$$

When the interface Σ is planar and we can separate the up and downgoing propagation character of the Green's functions and the scattered wave field at the boundary, then we can reduce equation (12) to

$$\begin{aligned} \Delta P(\mathbf{x}^R|\mathbf{x}^S) &= \int_{\Sigma} \frac{2}{\varrho(\mathbf{x})} \left(\partial_3 \Delta P(\mathbf{x}|\mathbf{x}^R) \right) G^0(\mathbf{x}|\mathbf{x}^S) dA \\ &\text{with } \{\mathbf{x}^R, \mathbf{x}^S\} \in \mathbb{D}', \end{aligned} \quad (13)$$

in which $\partial_3 \Delta P(\mathbf{x}|\mathbf{x}^R)$ is the reflection function of the difference wavefield and $G^0(\mathbf{x}|\mathbf{x}^S)$ represents the Green's function of the reference medium.

Difference data

In Figure 1 we show a plane-layer model with two disconnected reservoir layers with thicknesses of 25m and 50m, and top interfaces at a depth of 475m and 825m respectively.

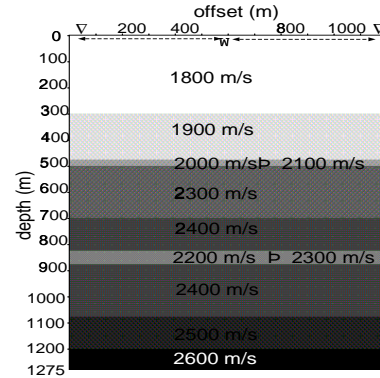


Fig. 1: reference and monitor model.

This model is used to create two time-lapse synthetic shotgatherers by means of a finite-difference program. The velocities for

4-D imaging

the reference and the monitor state are also shown in this figure as well as the shot and receiver positions. Synthetic data allows us to simulate complete repeatability of the two time-lapse experiments, an assumption which is of course not strictly valid in practice. Therefore changes between the two datasets are confined to the two reservoir layers (events 3 and 5). Figure 2 shows the reference shotgather at $t = t_0$ created by the finite-difference program. After subtracting the reference dataset from the monitor dataset at $t = t_1$ we obtain in Figure 3 the difference shotgather.

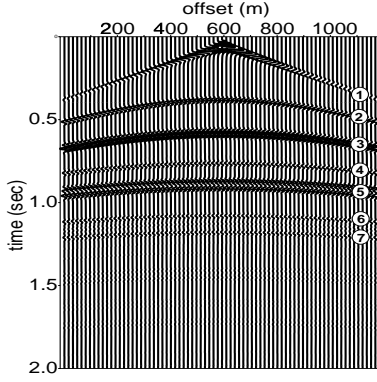


Fig. 2: reference shotgather.

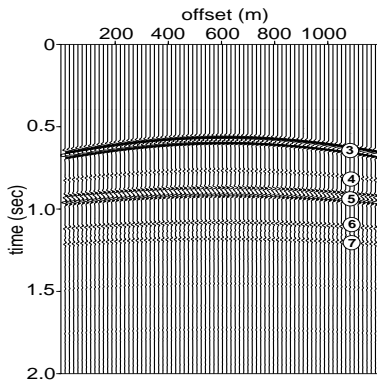


Fig. 3: difference shotgather.

In this figure we observe that after subtraction the first difference reflection can be identified with the boundary of the temporal contrast domain (Σ in equation (13)), being the top interface of the upper reservoir at 475m. The reflection from the first interface at 300m has disappeared because the spatial contrast has not changed in time. In a practical situation such a reflector can be used to assess the repeatability of the seismic experiment. Zero amplitude would imply complete repeatability whereas residual amplitude can be used as a measure for non-repeatability. Likewise

an amplitude matching procedure could be devised that should minimize the residual amplitude.

In Figure 3 we can see that all interfaces below the top interface of the upper reservoir are present in the difference shotgather as difference reflections. Interfaces which share the same spatial contrast in the reference and monitor state do not cancel completely after subtraction, meaning that not all difference reflections can be identified with temporal contrasts. They occur in the difference shotgather because the reflections in the monitor shotgather are shifted in time with respect to the reflections in the reference shotgather¹. The time-shift depends on the thickness of the temporal contrast and the contrast itself, and it is cumulative. The bottom interface of the upper reservoir (bottom event 3), event 4, and the top interface of the lower reservoir (top event 5) are shifted by an amount related to the velocity change in the upper reservoir layer. The time-shift of the bottom interface of the lower reservoir (bottom event 5) and events 6 and 7 is the sum of two time-shifts related with the velocity changes in the upper and the lower reservoir layers respectively. To be able to handle the time-shifts separately we propose a top-to-bottom approach which will be explained in the next section.

4-D redatuming and imaging

Our 4-D imaging scheme is based on the inversion of Equation (13) for the difference reflection (for the imaging see [5]). Therefore source and receivers should be positioned inside a domain in which no temporal contrasts have occurred. In this way the top boundary of a layered temporal contrast can be imaged using the velocities of the reference model in the Green's function $G^0(\mathbf{x}|\mathbf{x}^S)$. So with the source and receivers at the surface level (see Figure 1) the top interface of the upper reservoir is imaged correctly as can be seen in Figure 4 (top event 3). This last figure is created by imaging the entire difference dataset using the Green's function of the reference model. This procedure is equivalent to processing two time-lapse datasets separately with exactly the same processing parameters and subtracting the result, a common practice in time-lapse seismic processing.

The induced depth-shifts in Figure 4 at the bottom interface of the upper reservoir and at the layers below is used to calculate the associated velocity change. The same information is also present in the difference reflection of the top interface of the reservoir. Knowing the velocity change we are able to image the bottom interface of the upper reservoir layer correctly by redatuming source and receivers to this level (see [4]). The redatuming through the temporal contrast domain is performed for the reference and monitor state separately using the Green's function of the reference state (assumed to be known) and the calculated Green's function of the monitor state respectively. After redatuming below the top

¹Note that there is also a difference in amplitude due to the difference in transmission coefficients in the upper reservoir layer. However this effect is less pronounced and not important in the imaging procedure.

4-D imaging

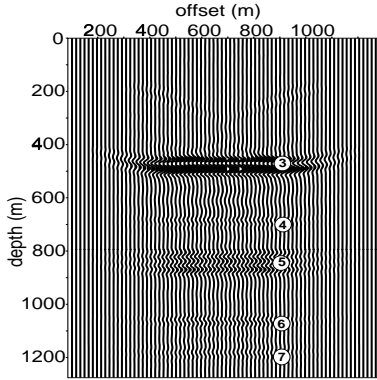


Fig. 4: erroneous difference image.

reservoir source and receivers are again inside a domain in which no temporal contrast have occurred and Equation (13) can be used again to image the region from the bottom boundary of upper reservoir layer to the top boundary of the lower reservoir layer. As a result of the redatuming of the source and receivers below the upper reservoir layer the depth shifts associated with this layer are removed from the difference data. This can be seen in Figure 5 in which the difference of a redatumed reference and monitor shotgather are shown with shot and receivers now at 600m, just below the upper reservoir layer. Comparing this figure with Figure 3 (source and receiver at 0m) we see that e.g. the interface at 700m (event 4) has disappeared in Figure 5 because in both states the propagation effect of the upper reservoir layer has been eliminated.

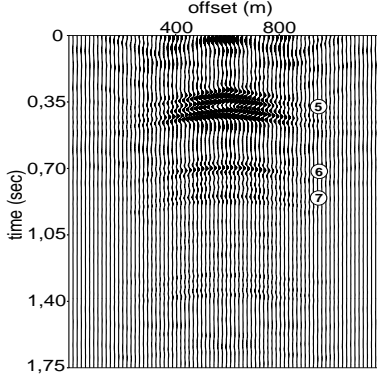


Fig. 5: difference redatuming at 600m.

Following the procedure as described above we can proceed by imaging the region from the bottom boundary of the lower reservoir layer to the end of the section. The end result is shown in Figure 6. Comparing this last figure with Figure 4 we observe that in Figure 6 the depth-shifts are eliminated and as a result the

events not associated with temporal contrast, events 4,6 and 7, are minimized.

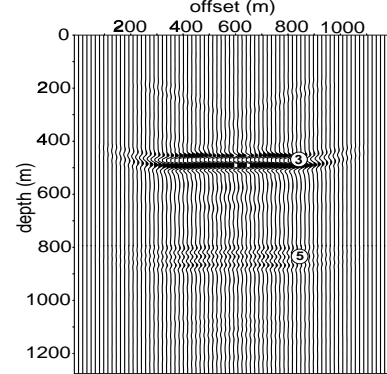


Fig. 6: correct difference image.

Conclusions

In this paper we have shown that the global form of the acoustic reciprocity theorem serves as a suitable tool to relate the two seismic measurements of a 4-D experiment. We restrict our analysis to compressibility contrasts only, while the inhomogeneous mass density remains the same in the two states. This restriction is commonly associated with velocity contrasts only. The volume integral of compressibility contrasts leads to an inversion approach, but after formulation this road is not further explored. On the other hand, the boundary integral formulation leads to an imaging procedure of the difference wave field. As a result the difference of the reflection operator between the two seismic experiments is mapped at every contrast boundary when performing a correct redatuming of the wave fields through the contrast domains.

References

- [1] Cruts, H. M. A., Groenenboom, J., Duijndam, A. J. W., and Fokkema, J. T., 1995, Experimental verification of stress-induced anisotropy: 65th Annual Internat. Mtg., Soc. Expl. Geophys., Expanded Abstracts, 894–897.
- [2] Fokkema, J. T., and van den Berg, P. M., 1993, Seismic applications of acoustic reciprocity: Elsevier, Amsterdam.
- [3] Nur, A., Tosaya, C., and V-Thanh, D., 1984, Seismic monitoring of thermal enhanced oil recovery processes: 54th Annual Internat. Mtg., Soc. Expl. Geophys., Expanded Abstracts, 118–121.
- [4] Wapenaar, C. P. A., and Berkhouw, A. J., 1989, Elastic wave field extrapolation: Elsevier Amsterdam.
- [5] Berkhouw, A. J., 1985, Seismic migration: Imaging of acoustic energy by wavefield extrapolation: Elsevier Amsterdam.